CRITICAL MAGNETIC FIELD FOR A SYMMETRIC QUANTUM WELL OR SINGLE BARRIER

Chi-Suan Wang
Institute of Electronics, National Chiao Tung University,
Hsinchu 30050, Taiwan, R.O.C.

Der-San Chuu
Department of Electro-Physics, National Chiao Tung University,
Hsinchu 30050, Taiwan, R.O.C.

(Revised September 27, 1993)

The energy spectra of a symmetric quantum well and single barrier within an in-plane magnetic field are exactly derived and the numerical results are calculated by iteration. A critical distance between the edge of electron spiral radius and the barrier boundary is introduced to describe the relation of well or barrier width and the critical magnetic field beyond which the Landau levels will dominate. We can predict by a simple equation when bulk Landau levels will dominate in the middle of the well or barrier region. A prediction of the critical magnetic field in the characteristics of electron state energy versus magnetic field strength for both quantum well and single barrier shows a good agreement.

In recent years, electro-magneto properties of a quasi two dimensional electron gas in quantum well semiconductor heterostructures have attracted a wide attention due to the possibility in high performance electronics of tunneling devices. The basic configuration of these quantum devices may be a single barrier[1-2], quantum well[3-4], double barrier[5-7], or multiple quantum well[8] structures. In these studies, the direction of the external applied magnetic field to the quantum devices were considered to be perpendicular, parallel or tilt to the growth direction. When a constant homogeneous magnetic field is applied perpendicular to the growth direction, the Landau levels of the confined electrons are formed and the energy spectrum becomes discrete. The fundamental study of the energy spectrum of an electron in a quantum well or single barrier structure is of considerable interest and will be helpful to realize the transport phenomena of the quantum devices. The electronic energy spectrum in a quantum well or single barrier of non- interacting electrons in a magnetic field tilted with respect to the growth direction have been studied for the case of a parabolic quantum well potential[9]. We concentrate in this paper on the effects of electronic energy levels in a quantum well and a single barrier under an in-plane magnetic field. Conceptually, one can expect that the energy spectrum of an electron confined in a narrow well depends critically on the well width. However as the well width is much larger than the magnetic length $l_B = \sqrt{\hbar/\mu\omega}$, which can be achieved by applying a sufficient strong magnetic field or with a physically wide quantum well, the electron orbits are governed by the Lorentz force semi-classically and will be constrained to a spiral motion along the magnetic lines. In this limit case, the electrons around the center of the well or barrier region are not affected by the potential barrier essentially, so the energy spectrum around this region will exhibit the main feature of the bulk Landau levels. On contrary, in the limit case of small magnetic field or physically narrow well or barrier width, because the orbital motion of electrons is reflected by both potential step barriers of quantum well or single barrier frequently, the energy levels will be dominated by the spatial quantization. When the well or barrier width is comparable to the magnetic length, the energy

0749-6036/93/010087+07 $08.00/0

levels will be quantized by the combined effects of the spatial confinement, the barrier height of quantum well or single barrier and Landau levels determined by the magnetic field B. In this situation, the classical skipping orbits are formed due to the spiral motion of the electrons reflected by only a single barrier or both barriers. Hence, it should be interesting to determine the critical condition when bulk Landau levels will dominate in the middle of the well or barrier region.

We consider a symmetric quantum well or single barrier structure with growth direction in $\hat{x}$. The external magnetic field is applied along $\hat{z}$- direction, i.e. $\vec{B} = (0, 0, B_0)$, which can be described by the vector potential $\vec{A} = (0, xB_0, 0)$. The Hamiltonian of an electron in such a system can be written as

$$H = \frac{(p_x^2 + p_z^2)}{2\mu} + \frac{(p_y + eB_0 x)^2}{2\mu} + V(x) \ , \qquad (1)$$

where μ is the effective mass of the electron and $V(x)$ is the well or barrier potential energy of the electron. The corresponding Schrödinger equation is given as $H\Psi\left(\vec{r}\right) = E_n \Psi\left(\vec{r}\right)$. Since the coordinates $\hat{y}$ and $\hat{z}$ are cyclic in H, thus the wave functions for the in-plane motion can be assumed as

$$\Psi\left(\vec{r}\right) = R(x)\ e^{i(k_y y + k_z z)} \ . \qquad (2)$$

Substituting $\Psi\left(\vec{r}\right)$ into the Schrödinger equation, we get the differential equation for $R(x)$:

$$\frac{d^2 R(x)}{dx^2} + \frac{\epsilon - V(x) - \mu\omega^2 (x + x_0)^2 / 2}{\hbar^2 / 2\mu} R(x) = 0. \quad (3)$$

Introducing the dimensionless variable $\xi = \sqrt{2}x/l_B$ with magnetic length $l_B = \sqrt{\hbar/\mu\omega}$, the Schrödinger equation can be written as

$$\frac{d^2 R(\xi)}{d\xi^2} + \left(\frac{\epsilon - V}{\hbar\omega} - \frac{1}{4}(\xi + \xi_0)^2\right) R(\xi) = 0. \quad (4)$$

In eq. (3) and (4), we define $\epsilon = E_n - p_z^2/2\mu$, $\omega = eB_0/\mu$, $x_0 = \hbar k_y / eB_0$ and dimensionless orbit center $\xi_0 = \sqrt{2}x_0/l_B = \sqrt{2} l_B k_y$. Now let $m + 1/2 = (\epsilon - V)/\hbar\omega$ and $z = \xi - \xi_0$, then eq. (4) can be expressed as the well known Weber's eq.

$$\frac{d^2 D_m(z)}{dz^2} + \left(\left(m + \frac{1}{2}\right) - \frac{z^2}{4}\right) D_m(z) = 0. \quad (5)$$

The solution of the Weber's eq. is

$$D_m(z) = \frac{\sqrt{\pi} e^{-\frac{z^2}{4}} 2^{\frac{m}{2}}}{\Gamma(1/2 - m/2)} F\left(-\frac{m}{2} \left|\frac{1}{2}\right| \frac{z^2}{2}\right)$$

$$- \frac{\sqrt{2\pi} z e^{-\frac{z^2}{4}} 2^{\frac{m}{2}}}{\Gamma(-m/2)} F\left(\frac{1-m}{2} \left|\frac{3}{2}\right| \frac{z^2}{2}\right) , \qquad (6)$$

where $\Gamma(x)$ is the Gamma function and $F(a\,|b|\,c)$ is the confluent hypergeometric function[10]. From the asymptotic properties of the Weber function[11], the general solution of eq. (4) can be expressed as following

$$R(z) = A D_m(z) + B D_m(-z) \ , \qquad (7)$$

where the coefficients A and B are the normalization constants.

To investigate the individual effect of magnetic field or barrier reflection, we first consider a single step barrier under an in-plane magnetic field. The step barrier potential $V(x)$ and well-behaved wave function $R(z)$ can be written respectively as

$$V(x) = \begin{cases} V_0 & , x \le x_1 \\ 0 & , x > x_1 \end{cases} ,$$

$$R(z) = \begin{cases} B_1 D_{m_1}(-z) & , z \le z_1 \\ A_2 D_{m_2}(z) & , z > z_1 \end{cases} .$$

Applying the continuity conditions of the wave function and its first derivative at boundary position $z_1 = \xi_1 - \xi_0$ and $m_1 = m_2 - V_0/\hbar\omega = \epsilon/\hbar\omega - 1/2 - V_0/\hbar\omega$ we get a nonlinear equation

$$D_{m_1}(-z_1) D'_{m_2}(z_1) + D_{m_2}(z_1) D'_{m_1}(-z_1) = 0 \ , \quad (8)$$

which depends only on two independent variables $\epsilon/\hbar\omega$ and dimensionless orbit center ξ_0. The characteristics of $\epsilon/\hbar\omega$ versus ξ_0 as shown in Fig. 1 (a), (b) and (c) are evaluated by using eq. (8) with iteration method. In Fig. 1 (a), one can see that in region A and B the orbit center is far away from the step barrier and the characteristics is totally dominated by bulk Landau levels except a shift of a constant barrier height V_0 in region B. This means in region A and B the cycloid motion of electrons is not affected by the barrier and the electrons do not see the potential barrier essentially. In region C, the cycloid motion of an electron reflected by the step barrier forms a skipping orbit and the energy levels are quantized to edge states and strongly depend on the potential barrier height V_0. The circles denote the critical orbit centers, beyond which the nth bulk Landau level ($(n + 1/2)\hbar\omega$) dominates totally. To describe the behavior of the parabolic increase of the critical orbit center, we introduce a critical distance ξ_c between the barrier boundary and the edge of electron cycloid motion as shown in Fig. 1 (d), beyond which electrons are not affected by the potential barrier and dominated by bulk Landau levels entirely. The relation between electron energy $\mu x_R^2 \omega^2/2$ and bulk Landau levels $(n + 1/2)\hbar\omega$ then can be written as

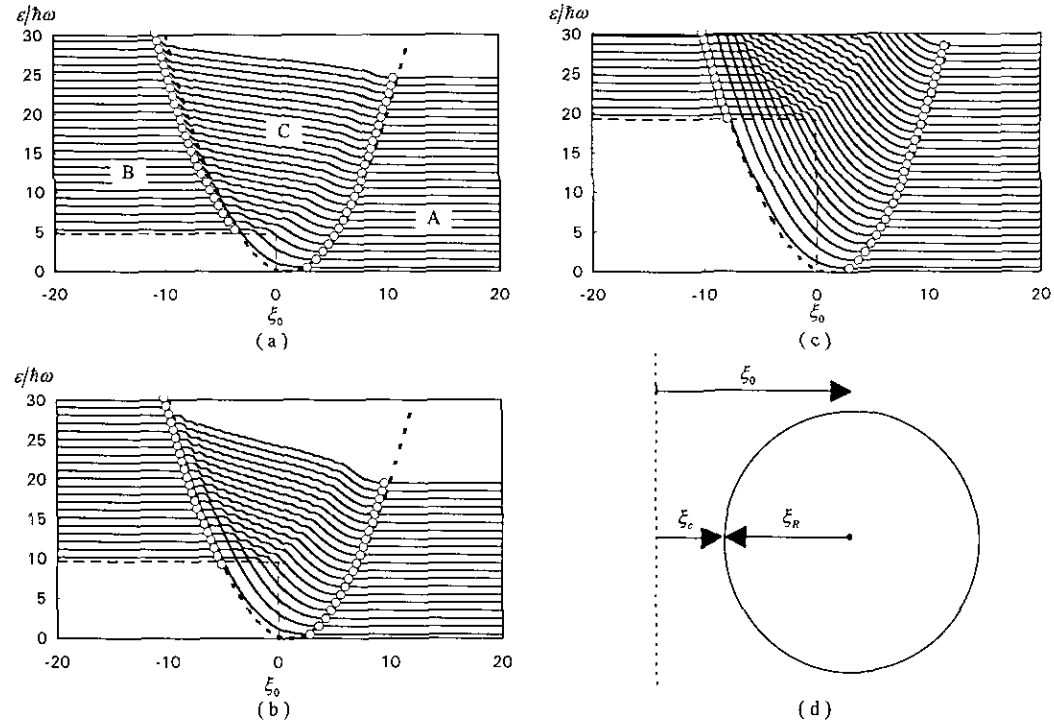

1. Fig. 1. Energy spectra in a single step potential barrier with in- plane magnetic field to be 10 $Tesla$ and barrier height to be (a) $V_0 = 4.813\hbar\omega$, (b) $V_0 = 9.625\hbar\omega$ and (c) $V_0 = 19.25\hbar\omega$. The dimensionless orbit center is defined as $\xi_0 = \sqrt{2}x_0/l_B = \sqrt{2}l_B k_y$. Energy levels in region A and B are dominated by bulk Landau levels with constant potential elevation. Semi-classically, in region C the cycloid motion of an electron is reflected by the step barrier and forms a skipping orbit. (d) Schematic of the relative positions among critical distance ξ_c, orbit center ξ_0 and radius of the electron cycloid motion ξ_R away from a single step barrier(dashed line). The dashed lines in (a), (b) and (c) represent the guide lines of predicted critical points and the circles are actual critical points.

$$\frac{1}{2}\mu x_R^2\,\omega^2 = \frac{1}{4}\xi_R^2\,\hbar\omega = \epsilon = \left(n+\frac{1}{2}\right)\hbar\omega\,, \qquad (9)$$

where x_R is the radius of electron spiral motion and $\xi_R = \sqrt{2}x_R/l_B$. Substituting $\xi_R = \xi_0 - \xi_c$ into eq. (9), we have a relation between ϵ and ξ_0

$$\epsilon = \frac{1}{4}(\xi_0 - \xi_c)^2\,\hbar\omega \qquad (10)$$

to determine when bulk Landau levels will dominate totally. The critical distance ξ_c is calculated to be 1.1 by using least squares fitting the curve formed by the circles in Fig. 1 (a), (b) and (c) with eq.(10). One can expect that if the physical distance between the edge of electron cycloid motion and the step barrier is larger than 0.78 l_B the electron is not affected by the potential barrier.

Fig. 1 (a), (b) and (c) show the energy spectra of a step barrier with different potential heights. The thick dashed lines are the guide lines of the critical orbit

centers predicted by eq. (10). The circles denote the actual critical orbit centers, one can see that the predictions are accurately close to the actual ones. One also see that the characteristics dominated by bulk Landau levels in region A are not affected by the magnitude of the step barrier potential height. In region B, the bulk Landau levels are shifted with a constant potential height V_0 and the critical orbit centers in region B also follow the guide line predicted by eq. (10). In region C, one can see the number of edge states increases due to the increasing of the step potential height.

Now let us consider a symmetric quantum well with an in-plane homogeneous magnetic field in $\hat{z}$- direction. The step barrier potential $V(x)$ and the well-behaved wave function $R(z)$ can be written respectively as

$$V(x) = \begin{cases} V_0 & , x \le x_1 \\ 0 & , x_1 < x < x_2 \\ V_0 & , x \ge x_2 \end{cases} ,$$

$$R(z) = \begin{cases} B_1 D_{m_1}(-z) & , z \le z_1 \\ A_2 D_{m_2}(z) + B_2 D_{m_2}(-z) & , z_1 < z < z_2 \\ A_3 D_{m_3}(z) & , z \ge z_2 \end{cases}$$

The well width x_w is defined by $x_2 - x_1$. Applying the continuity conditions of the wave functions and its first derivative in both boundaries z_1 and z_2, we have

$$\begin{bmatrix} D_{m_1}(-z_1) & -D_{m_2}(z_1) & -D_{m_2}(-z_1) & 0 \\ -D'_{m_1}(-z_1) & -D'_{m_2}(z_1) & D'_{m_2}(-z_1) & 0 \\ 0 & D_{m_2}(z_2) & D_{m_2}(-z_2) & -D_{m_3}(z_2) \\ 0 & D'_{m_2}(z_2) & -D'_{m_2}(-z_2) & -D'_{m_3}(z_2) \end{bmatrix} \times \begin{bmatrix} B_1 \\ A_2 \\ B_2 \\ A_3 \end{bmatrix} = 0 , \quad (11)$$

where $z_i = \xi_i - \xi_0$ and $\xi_i = \sqrt{2} x_i / l_B$ $i = 1, 2$. For nontrivial solutions of coefficients, we have a nonlinear equation defined by

$$\begin{vmatrix} D_{m_1}(-z_1) & -D_{m_2}(z_1) & -D_{m_2}(-z_1) & 0 \\ -D'_{m_1}(-z_1) & -D'_{m_2}(z_1) & D'_{m_2}(-z_1) & 0 \\ 0 & D_{m_2}(z_2) & D_{m_2}(-z_2) & -D_{m_3}(z_2) \\ 0 & D'_{m_2}(z_2) & -D'_{m_2}(-z_2) & -D'_{m_3}(z_2) \end{vmatrix} = 0 . \quad (12)$$

Since the quantum numbers m_1 and m_3 can be expressed in terms of $m_2 (= \epsilon/\hbar\omega - 1/2)$, as $m_i = m_2 + V_0/\hbar\omega$, i = 1 and 3, therefore, eq. (12) depends only on two independent variables $\epsilon/\hbar\omega$ and ξ_0. The characteristics of $\epsilon/\hbar\omega$ and ξ_0 can then be evaluated by iteration method as shown in Fig. 2 (a) and (b). The major difference between a wide well (Fig. 2 (a)) and a narrow one (Fig. 2 (b)) is the energy levels in the well region. In wide well case the energy levels in the middle of the well region are dominated by bulk Landau levels and the lower lying states exist a wider range of ξ_0 dominated by bulk Landau levels due to low energy and small cycloid radius. As the well width reduces, the edge of the spiral motion is reflected by both potential barriers and electron in this region forms a skipping orbit. One can see that the elevation of the ground state in the well region due to the combined effect of spatial confinement and edge states in narrow well case as shown in Fig. 2 (b). To investigate when the bulk Landau level dominates in the middle of the well region ($\xi_0 = 0$), we treat the well potential distribution as the superposition of two single step subsystems. Fig. 2 (c) shows the relative position of the maximum electron cycloid radius ξ_R, critical distance ξ_c and well width ξ_w, when the bulk Landau level dominates in the middle of the well region. The relation between the electron energy levels and bulk Landau levels can be expressed the same as eq.(9). Substituting $\xi_R = \xi_w/2 - \xi_c$, $\xi_0 = 0$ and $\xi_w = \sqrt{2} x_w / l_B$ into eq.(9), we have a relation between critical magnetic field B_{cw} for a symmetric well and physical well width x_w

$$B_{cw} = \frac{2\hbar}{e} \left(2\sqrt{(n + 1/2)} + \xi_c \right)^2 x_w^{-2} , \quad (13)$$

where n is the quantum number of bulk Landau levels. For a given symmetric quantum well width, one can use eq. (13) to predict the critical magnetic field, beyond which the nth bulk Landau level will exist in the middle of the well region. Fig. 2 (d) shows the electronic energy levels versus the magnetic field strength for the first four levels under the condition of $\xi_0 = 0 (k_y = 0)$ with well width to be 1200 $\mathring{A}$ and the same potential height as Fig. 2 (a) and (b). As the strength of magnetic field decreases, the state energy also decreases until approaches to limit values for zero magnetic field (closed circles in Fig. 2 (d)). The closed triangles shown in Fig. 2 (d) represent the state energies under critical magnetic fields, beyond which the bulk Landau levels will dominate. If magnetic field exceeds the critical field B_{cw} in each band, the bulk Landau levels will dominate for a wider range of ξ_0, otherwise the energy levels in the well region are affected by the combined effect of the spatial and magneto confinements. The dashed lines in Fig. 2 (d) represent the corresponding bulk Landau levels. The circles shown in Fig. 2 (d) represent the predicted critical points by eq.(13). One can see that the energy spectrum in the middle of the well region is dominated by bulk Landau levels, as the magnetic field is larger than the critical magnetic field and the prediction (circles in Fig. 2 (d)) shows a good agreement.

Finally, we consider a single quantum barrier with growth direction in $\hat{x}$ under an in-plane homogeneous magnetic field in $\hat{z}$- direction with potential distribution

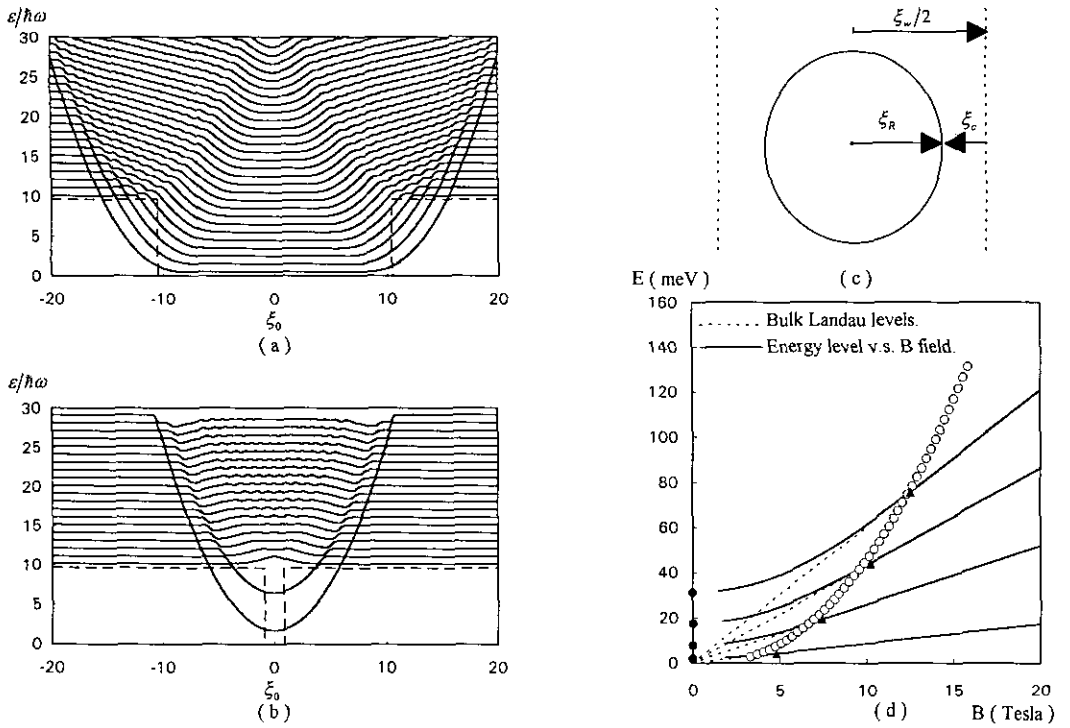

2. Fig. 2. Energy spectra in a symmetric quantum well with in- plane magnetic field to be 10 *Tesla* and well width ξ_w to be (a) 1200 $\mathring{A}$ (b) 100 $\mathring{A}$ respectively and barrier height $V_0 = 166.3$ meV. (c) Schematic of the relative positions among critical distance ξ_c, well width ξ_w and maximum radius of the electron cycloid motion ξ_R inside a symmetric quantum well(dashed lines). The dimensionless orbit center is defined as $\xi_0 = \sqrt{2}x_0/l_B = \sqrt{2}l_B k_y$. (d) Energy levels with the variation of in-plane magnetic field with well width 1200 $\mathring{A}$ and the same potential height as (a). The closed triangles represent the critical magnetic field for the first four bands, beyond which bulk Landau levels dominate. The closed circles represent the confined states with zero external magnetic field.

$$V(x) = \begin{cases} 0 & , x \le x_1 \\ V_0 & , x_1 < x < x_2 \\ 0 & , x \ge x_2 \end{cases} .$$

The barrier width x_b is defined by $x_2 - x_1$. Follow the same derivation procedure and suitable boundary conditions, the characteristics of $\epsilon/\hbar\omega$ and ξ_0 can be evaluated by iteration method as shown in Fig. 3 (a) and (b) with different barrier widths. The major difference between a wide quantum barrier (Fig. 3 (a)) and a narrow one (Fig. 3 (b)) is the energy levels in the barrier region. In wide barrier case shown in Fig. 3 (a), the energy levels in the middle of the barrier region are dominated by bulk Landau levels with a constant shift of step potential height V_0 and the lower lying states exist a wider range of ξ_0 dominated by bulk Landau level due to low energy and small cycloid radius. In the narrow barrier case shown in Fig. 3 (b), one can see that the energy lowering of the ground state in the middle of barrier due to the combined effect of spatial confinement and edge states in a narrow barrier width. To investigate when the bulk Landau level dominates in

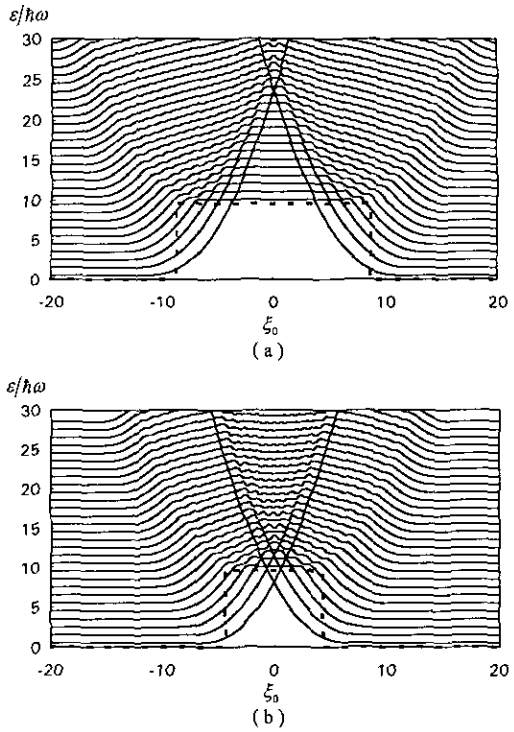

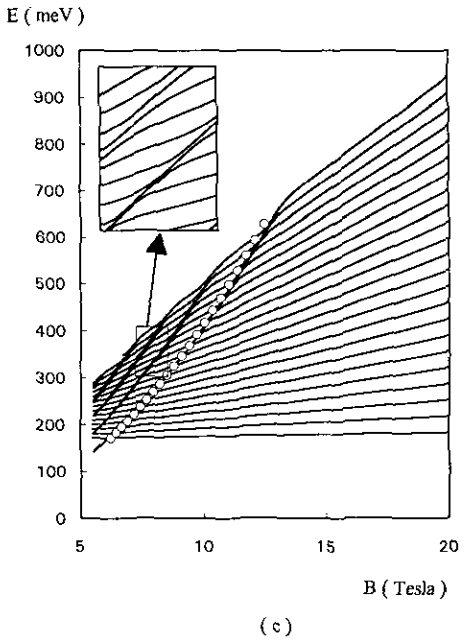

3. Fig. 3. Energy spectra in a single quantum barrier with in-plane magnetic field to be 10 *Tesla* and barrier width ξ_b to be (a) 1000 $\mathring{A}$ (b) 500 $\mathring{A}$ respectively and barrier height V_0 = 166.3 meV. The dimensionless orbit center is defined as $\xi_0 = \sqrt{2}x_0/l_B = \sqrt{2}l_B k_y$. (c) Energy levels with the variation of in-plane magnetic field with the same potential configuration as (a). The circles represent the predicted critical magnetic field, beyond which bulk Landau levels dominate. One can see the energy lowering for ground states at small magnetic field.The inset shows the magnified characteristics around the crossing points.

the middle of the barrier region ($\xi_0 = 0$), we derive the relation between critical magnetic field B_{cb} for quantum barrier *with physical barrier width* x_b. *Considering the* potential barrier height V_0 with similar derivation procedure as the quantum well case, *the relation among the* electron energy $\mu x_R^2 \omega^2/2$, potential barrier height V_0 and bulk Landau level $(n + 1/2)\,\hbar\omega$ can then be expressed as

$$\frac{1}{2}\mu x_R^2\,\omega^2 = \frac{1}{4}\xi_R^2\,\hbar\omega = \left(n + \frac{1}{2}\right)\hbar\omega + V_0\,. \qquad (14)$$

Then the relation between critical magnetic field B_{cb} for single quantum barrier and physical barrier width x_b can be expressed as

$$B_{cb} = \frac{2\hbar}{e}\left(2\sqrt{(n + 1/2) + V_0/\hbar\omega} + \xi_c\right)^2 x_b^{-2}. \qquad (15)$$

Eq. (15) is a nonlinear equation for magnetic field B_{cb} through the term of $\hbar\omega$ in the right hand side and critical magnetic field B_{cb} should be calculated by iteration method. One can also find that eq. (15) depends on the barrier height V_0, which is a significant difference compared with the quantum well case. Fig. 3. (c) shows the electronic energy levels versus the magnetic field strength under the condition of $\xi_0 = 0\,(k_y = 0)$ with the same potential configuration as Fig. 3 (a). As the strength of magnetic field decreases, one can see that *the state energy* also decreases and the energy lowering

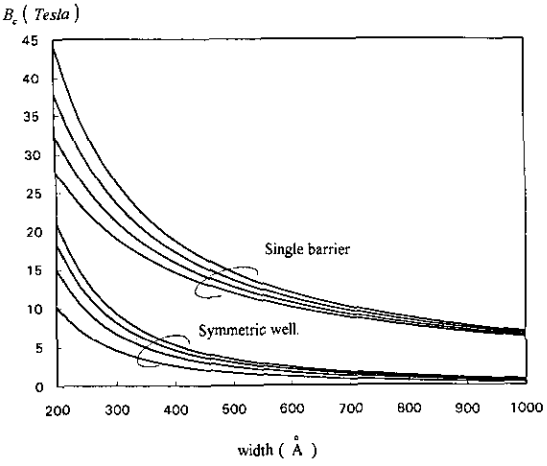

4. Fig. 4. Characteristics of critical magnetic field $B_{cw,b}$ versus well or barrier width for first four energy states. Due to the strong dependency of the barrier height, the calculated critical magnetic field for barrier case is larger than that of the well case.

occurs. Using the same critical space $\xi_c = 1.1$ and barrier width x_w, one can predict the critical magnetic field B_{cb} for each band. The circles in Fig. 3 (c) shows the critical points predicted by eq. (15), beyond which one can see that the energy spectrum is dominated by the bulk Landau levels. Fig. 4 shows the characteristics of critical magnetic field versus well or barrier width with the first four states by eq. (13) and (15). One can see that for a fixed width the critical magnetic field of single barrier is larger than that of the quantum well. This is due to the dependence of the barrier height and the nonlinear property of the magnetic field in eq.(15).

In summary, we discussed in this paper the critical magnetic field for both symmetric well and single quantum barrier with different well (barrier) width, beyond which the bulk Landau level dominates in the center of the quantum well or barrier. The interactions between the electron and the barrier in a single step barrier are classified to explain the classical behavior in the energy spectrum of a symmetric well and single barrier. It is shown that a critical distance ξ_c between the edge of electron spiral radius and the barrier boundary can be used to describe the relation of the critical magnetic field and well (barrier) width, with which one can use to accurately predict when bulk Landau levels will dominate in the middle of the well or barrier region. It is also found that in a quantum barrier the critical magnetic field strongly depends on the barrier height V_0, while in well case the critical magnetic is independent of the barrier height. The behavior of the bulk Landau level within a wide well or barrier and the elevation of the ground state in a narrow well or the energy lowering of the ground state in a narrow barrier are explained.

Acknowledgement- This work is partially supported by National Council of Science of Taiwan.

References

1. L.A. Cury, A. Celeste and J.C. Portal, Phys. Rev. B **39** 8760 (1989).
2. T.M. Fromhold, F.W. Sheard and G.A. Toombs, Surface Science **228** 1250 (1990).
3. A.B. Henriques and E.C. Valadares, Superlattices and Microstructures **10** 187 (1991).
4. H.R. Lee, H.G. Oh, Thomas F. George and C.I. Um, J. Appl. Phys. **66** 2442 (1989).
5. S. Ben Amor, J.J.L. Rascol, K.P. Martin, R.J. Higgins, R.C. Potter and H. Hier, Phys. Rev. B **41** 7860 (1990).
6. M.L. Leadbeater, E.S. Alves, L. Eaves, M. Henini, O.H. Hughes, A.C. Celeste and J.C. Portal, Superlattices and Microstructures **6** 63 (1989).
7. L. Brey, G. Platero and C. Tejedor, Superlattices and Microstructures **5** 531 (1989).
8. H. Schneider, K. von Klitzing and K. Ploog, Superlattices and Microstructures **5** 383 (1989).
9. O Kühn and P E Selbmann, Semicond. Sci. Technol. **6** 1181 (1991).
10. I.S. Gradshteyn, I.M. Ryzhik, **Table of Integrals, Series and Products**. (Academic Press Inc.) 1058 (1965).
11. P.M. Morse and H. Feshbach, **Methods of Theoretical Physics**, (Mcgraw-Hill Book Company, Inc.) 1403. (1953)